

Dynamic behavior of a railway track under a moving wheel load modelled as a sinusoidal pulse

Nouzha Lamdouar, Chakir Tajani and Mohammed Touati

Abstract. The aim of this paper is to evaluate the train/track induced loads on the substructure by modelling the wheel, at each instant, as a moving sinusoidal pulse applied in a very short period of time. This assumption has the advantage of being more realistic as it reduces the impact of time on the load definition. To that end, mass, stiffness, and dumping matrices of an elementary section of track will be determined. As a result, the equations of motion of a section of track subjected to a sinusoidal pulse and a rectangular pulse respectively is concluded. Two numerical methods of resolution of that equation, depending on the nature of the dumping matrix, will be presented. The computation results will be compared in order to conclude about the relevance of that load model. This approach is used in order to assess the nature and the value of the loads received by the substructure.

1 Introduction

Various theoretical and experimental researches have been performed in order to assess train/track induced loads on the substructure. Mohammed Touati and al. [1] determined the loads induced by a non-linear 3D multi-body modelled train on the track with taking into account wheel/rail contact properties and track irregularities. Yang Xinwen and al. [2]

MSC 2020: 74S05, 37M05, 74-10, 37N30

Keywords: Dynamic properties, Finite elements modelling, Railway track dynamics, Sinusoidal pulse load.

Affiliation:

Nouzha Lamdouar – Civil Department, Mohammadia School of Engineers, Mohammed V University, Morocco

E-mail: nlamdouar@gmail.com

Chakir Tajani – Department of Mathematics, Polydisciplinary Faculty of Larache, Abdelmalek Essaadi University, Morocco

E-mail: chakir_tajani@hotmail.fr

Mohammed Touati – Civil Department, Mohammadia School of Engineers, Mohammed V University, Morocco

E-mail: mohammed.touati87@gmail.com

concluded, through a vehicle-track-subgrade coupling dynamic theory and finite element method, about the train/track induced loads on each layer of the substructure. As an experimental study, Al Shaer and al. [3] presented the dynamic behavior of a portion of ballasted railway track subjected to cyclic loads in substitution of a moving wheelset. In conclusion, the dynamics behavior of the substructure is widely studied in the literature ([4], [5], [6], [7], [8]) based on the train/track coupling model.

Actually, even if modelling a wheel load as a rectangular pulse is a common assumption, real measurements don't show the same shape. In fact, ONCF (Moroccan railway network manager) has many tools that record wheel pulse like GOTCHA. This system shows that the shape of the load has never been rectangular, but it's more likely compared to a sinusoidal pulse. Then, this paper deals with evaluating train/track induced loads on the substructure by proposing a new approach when it comes to modelling the shape of the wheel impact. Indeed, it's common to consider a moving load as a rectangular impulse applied on the nodes of a mesh structure in each period of time depending on signal sampling. This paper shows that assuming the wheel load as a sinusoidal pulse may reduce the impact of the period of time of its application and, consequently, minimize the loads induced on the substructure oversized by the common assumption. In that matter, a finite element model of the track will be presented and the numerical results will be compared.

2 Track elementary section modeling

2.1 Determination of mass, stiffness et dumping matrices

Let's assume a portion of ballasted track composed of two elements of rail considered as a continuous Euler-Bernoulli beam, fixed to two sleepers by a couples of springs/dampers representing the railpads. The ballast is modelled as a couples of springs/dampers under each sleeper (Figure 1).

The displacement vector is written as:

$$U = [u_1, \theta_1, u_2, \theta_2, u_3, \theta_3, u_{T1}, u_{T2}]$$

The effective mass and the stiffness matrices of an element of rail [9], are given by:

$$M_r = (\rho_r A_r L / 420) \begin{bmatrix} 156 & 22L & 54 & -13L & 0 & 0 \\ 22L & 4L^2 & 13L & -3L^2 & 0 & 0 \\ 54 & 13L & 312 & 0 & 54 & -13L \\ -13L & -3L^2 & 0 & 8L^2 & 13L & -3L^2 \\ 0 & 0 & 54 & 13L & 156 & -22L \\ 0 & 0 & -13L & -3L^2 & -22L & 4L^2 \end{bmatrix}$$

$$K_r = (E_r I_r / L^3) \begin{bmatrix} 12 & 6L & -12 & 6L & 0 & 0 \\ 6L & 4L^2 & -6L & 2L^2 & 0 & 0 \\ -12 & -6L & 24 & 0 & -12 & 6L \\ 6L & 2L^2 & 0 & 8L^2 & -6L & 2L^2 \\ 0 & 0 & -12 & -6L & 12 & -6L \\ 0 & 0 & 6L & 2L^2 & -6L & 4L^2 \end{bmatrix}$$

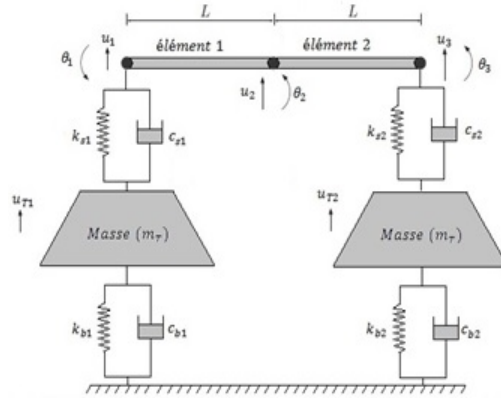


Figure 1: Elementary track modelling

where ρ_r is the density of the rail, A_r is the surface of the rail section, E_r is Young modulus, and I_r is the rail moment of inertia. The dumping matrix of the rail is obtained as a linear combination of mass and stiffness matrices by assuming that the displacements u_1 and u_3 are completely dumped by the effect of railpads.

Therefore, the dumping matrix is written as:

$$C_r^* = a_0 \cdot M_r^* + a_1 \cdot K_r^*$$

where,

$$M_r^* = (\rho_r A_r L / 420) \begin{bmatrix} 4L^2 & 13L & -3L^2 & 0 \\ 13L & 312 & 0 & -13L \\ -3L^2 & 0 & 8L^2 & -3L^2 \\ 0 & 13L & -3L^2 & 4L^2 \end{bmatrix}$$

$$K_r^* = (E_r I_r / L^3) \begin{bmatrix} 4L^2 & -6L & 2L^2 & 0 \\ -6L & 24 & 0 & 6L \\ 2L^2 & 0 & 8L^2 & 2L^2 \\ 0 & 6L & 2L^2 & 4L^2 \end{bmatrix}$$

a_0 and a_1 are concluded from the equation:

$$\begin{bmatrix} a_0 \\ a_1 \end{bmatrix} = (2\omega_1\omega_2 / (\omega_2^2 - \omega_1^2)) \begin{bmatrix} \omega_2 & -\omega_1 \\ -1/\omega_2 & 1/\omega_1 \end{bmatrix} \begin{bmatrix} \zeta_1 \\ \zeta_2 \end{bmatrix}$$

where ω_i^2 , ($i = 1, 2$) are the eigenvalues associated to the vibration of the rail described by the matrices M_r^* and K_r^* , and ζ_i , ($i = 1, 2$) are the dumping ratios according to the first and second modes.

In one hand, the equation of motion of the rail is written as:

$$M_r \ddot{U}^* + C_r \dot{U}^* + K_r U^* = F \quad (1)$$

Symbol	Quantity	Value
ρ_r	Rail density (kg/m ³)	7850
A_r	Rail section surface (cm ²)	76.70
E_r	Young modulus of the rail (GPa)	210
I_r	Rail moment of inertia (cm ⁴)	3038.6
m_T	Sleeper mass (kg)	90.84
k_s	Railpad stiffness (MN/m)	90
c_s	Railpad damping (kN.s/m)	30
k_b	Ballast stiffness (MN/m)	25.5
c_b	Ballast damping (kN.s/m)	40
ζ	Rail dumping ratio	5%

Table 1: Track properties

where C_r is the transformation of the matrix C_r^* in the base U^* , and U^* is defined by:

$$U^* = [u_1, \theta_1, u_2, \theta_2, u_3, \theta_3]$$

F is given by:

$$F = \begin{bmatrix} -k_s(u_1 - u_{T1}) - c_s(\dot{u}_1 - \dot{u}_{T1}) \\ 0 \\ 0 \\ 0 \\ -k_s(u_3 - u_{T3}) - c_s(\dot{u}_3 - \dot{u}_{T3}) \\ 0 \end{bmatrix}$$

In the other hand, the equations of motion of the sleepers are written as:

$$\begin{cases} m_T \ddot{u}_{T1} = k_s(u_1 - u_{T1}) + c_s(\dot{u}_1 - \dot{u}_{T1}) - k_b u_{T1} - c_b \dot{u}_{T1} \\ m_T \ddot{u}_{T2} = k_s(u_3 - u_{T2}) + c_s(\dot{u}_3 - \dot{u}_{T2}) - k_b u_{T2} - c_b \dot{u}_{T2} \end{cases} \quad (2)$$

From (1) and (2), we may conclude about the equation of motion of the track elementary section as it's modelled. It's written as:

$$M\ddot{U} + C\dot{U} + KU = 0$$

where M , C and K are the mass, dumping, and the stiffness of the track elementary section respectively.

2.2 Numerical application

Let's assume a track elementary section characterized by the data given in table 1 (we can refer to ([10], [11], [12])).

The figure 2 illustrates the evolution of natural frequencies according to vibration modes. It shows that:

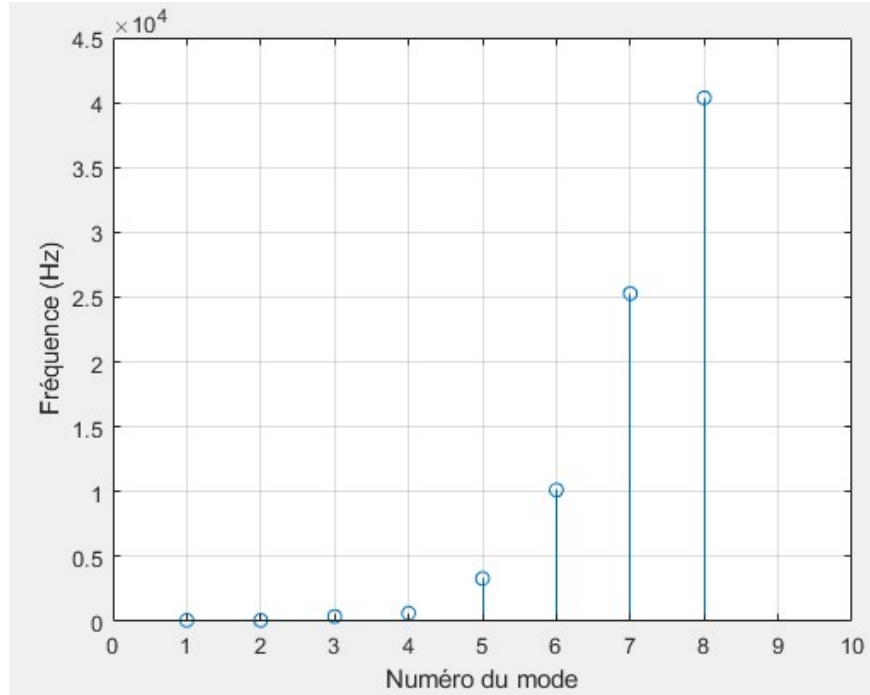


Figure 2: Natural frequencies of an elementary track section

- The frequencies of the 1st and 2nd modes correspond to a movement in phase between rail and sleepers. It's equal to 81.62 Hz;
- The frequency of the 3rd mode corresponds to a movement in opposition of phase between rail and sleepers. It's equal to 381.1 Hz.

3 Track response to a rectangular and a sinusoidal pulses

3.1 Description of the studied track

Let's assume a section of track composed of N track elementary sections subjected to an external load F as it's shown in figure 3.

The number of degrees of freedom is given by:

$$N_{dof} = 8N - 3(N - 1)$$

The displacement vector is written as:

$$U = \begin{bmatrix} \vdots \\ u_{j,k} \\ \vdots \end{bmatrix}$$

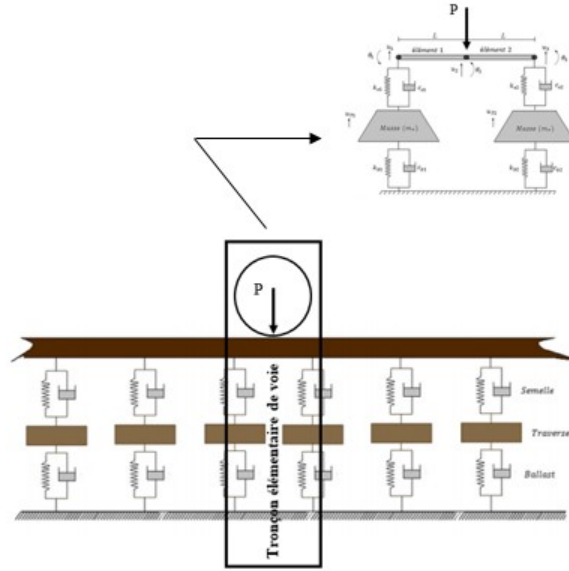


Figure 3: Track section modelling

where,

$$\begin{cases} u_{j,k} = u_{j,k}^* & \text{where } k \in [1, 8] & \text{if } j = 1 \\ u_{j,k} = u_{j,k}^* & \text{where } k \in [3, 4, 5, 6, 8] & \text{if } j \neq 1 \end{cases}$$

and,

$$U_j^* = [u_{j,1}, \theta_{j,1}, u_{j,2}, \theta_{j,2}, u_{j,3}, \theta_{j,3}, u_{j,T1}, u_{j,T2}]$$

j refers to the element's number.

The mass, stiffness and dumping matrices in the base U are obtained by assembling those of a track elementary section determined earlier.

The vector of loads is defined by:

$$F = \begin{bmatrix} \vdots \\ f_j \\ \vdots \end{bmatrix}$$

where,

$$\begin{cases} N \text{ is even} & \begin{cases} N = 2 & \begin{cases} f_j = P & \text{if } j = 5 \\ f_j = 0 & \text{else} \end{cases} \\ N \neq 2 & \begin{cases} f_j = P & \text{if } j = (5N/2) + 1 \\ f_j = 0 & \text{else} \end{cases} \end{cases} \\ N \text{ is uneven} & \begin{cases} f_j = P & \text{if } j = (5(N + 1)/2) - 1 \\ f_j = 0 & \text{else} \end{cases} \end{cases}$$

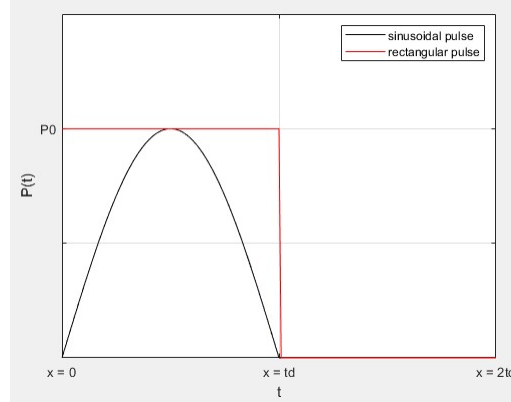


Figure 4: Sinusoidal and rectangular pulses over a period of t_d

P is a rectangular or a sinusoidal load given as:

- Sinusoidal pulse:

$$\begin{cases} P = P_0 \sin \omega t & \text{if } t \leq t_d \\ P = 0 & \text{else} \end{cases}$$

- Rectangular pulse:

$$\begin{cases} P = P_0 & \text{if } t \leq t_d \\ P = 0 & \text{else} \end{cases}$$

Its shape is shown in the figure 4.

3.2 Description of the methods of resolution

The dynamic behavior of the section of track may be analyzed by modal superposition if the dumping matrix verifies orthogonality properties. That method is used in particular for an undumped system. In that case, the equation of motion is reduced to:

$$M\ddot{U} + KU = F.$$

Let's assume that ω_i^2 are the eigenvalues associated to the track vibration. We note $\{\phi_i\}$ the normalized eigenvectors related to ω_i^2 . Therefore, the equation of motion is written as:

$$\ddot{Z} + \text{diag}(\omega_i^2)Z = \phi^T F \quad (3)$$

where $\text{diag}(\omega_i^2)$ is a diagonal matrix of the eigenvalues and:

$$U = \Phi.Z$$

The system of equations (3) is uncoupled where each equation is written as:

$$\ddot{z}_i + \omega_i^2 z_i = \Phi_{j,i} P(t)$$

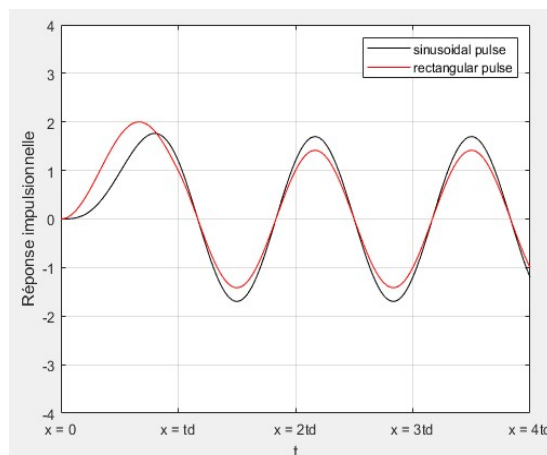


Figure 5: $z(t)$ response to a rectangular and sinusoidal pulse $t_d/T = 0.75$

The resolution of that equation is given by DUHAMEL integral:

$$z_i(t) = (1/\omega_i) \int_0^t \Phi_{j,i} P(\tau) \sin \omega_i(t - \tau) d\tau$$

Therefore, the solution for a sinusoidal pulse load is given as:

$$z_i(t) = \begin{cases} (\Phi_{j,i} P_0 / \omega_i^2) \cdot (1 / (1 - \beta^2)) (\sin \omega t - \beta \sin \omega_i t) & \text{if } t \leq t_d \\ (\dot{z}_i(t_d) / \omega_i) \sin \omega_i(t - t_d) + z_i(t_d) \cos \omega_i(t - t_d) & \text{if } t \geq t_d \end{cases}$$

where,

$$\beta = \omega / \omega_i$$

and the solution for a rectangular pulse load is given as:

$$z_i(t) = \begin{cases} (\Phi_{j,i} P_0 / \omega_i^2) (1 - \cos \omega_i t) & \text{if } t \leq t_d \\ (\Phi_{j,i} P_0 / \omega_i^2) (\cos \omega_i(t - t_d) - \cos \omega_i t) & \text{if } t \geq t_d \end{cases}$$

The figure 5 shows the response $z(t)$ to a sinusoidal and a rectangular pulse. It's obvious that in the forced phase, the maximum rectangular response is higher than the maximum sinusoidal response.

In general, the dumping matrix doesn't verify the orthogonality characteristics. Therefore, the modal superposition method is substituted by the following method.

The equation of motion can be written as:

$$\ddot{Z} + \phi^T C \phi \dot{Z} + \text{diag}(\omega_i^2) \cdot Z = \phi^T F \quad (4)$$

where $\text{diag}(\omega_i^2)$ and ϕ are defined earlier. Knowing that:

$$\dot{Z} - \dot{Z} = 0 \quad (5)$$

(4) and (5) could be written as:

$$\dot{Y} = D.Y + F^* \quad (6)$$

where,

$$Y = \begin{bmatrix} Z \\ \dot{Z} \end{bmatrix}, \quad D = A^{-1}B, \quad F^* = A^{-1} \begin{bmatrix} \phi^T F \\ 0 \end{bmatrix}$$

and,

$$A = \begin{bmatrix} \phi^T C \phi & I \\ I & 0 \end{bmatrix}, \quad B = \begin{bmatrix} \text{diag}(\omega_i^2) & 0 \\ 0 & -I \end{bmatrix}$$

Let's assume that $\{\lambda_i\}$ are the eigenvalues associated to the matrix D . We note $\{\psi_i\}$ the normalized eigenvectors related to $\{\omega_i^2\}$. We define $X(t)$ as:

$$Z = \psi.X$$

The equation (6) is written as:

$$\dot{X} = \text{diag}(\lambda_i).X + \psi^{-1}F^* \quad (7)$$

The system of equations (7) is uncoupled where each equation is written as:

$$\dot{x}_i(t) = a_i.x_i(t) + b_i.P \quad (8)$$

where,

$$a_i = \lambda_i \quad \text{and} \quad b_i = \chi_i$$

and,

$$\chi = \psi^{-1} \begin{bmatrix} \phi^T & 0 \\ 0 & 0 \end{bmatrix}$$

The resolution of the equation (8) gives:

- Sinusoidal pulse:

$$x_i(t) = \begin{cases} \frac{b_i P \omega}{a_i^2 + \omega^2} e^{a_i t} - \frac{a_i b_i P}{a_i^2 + \omega^2} \sin \omega t - \frac{b_i P \omega}{a_i^2 + \omega^2} \cos \omega t & \text{if } t \leq t_d \\ x_i(t_d) e^{a_i(t-t_d)} & \text{if } t \geq t_d \end{cases}$$

- Rectangular pulse:

$$x_i(t) = \begin{cases} (bP/a)(e^{a_i t} - 1) & \text{if } t \leq t_d \\ x_i(t_d) e^{a_i(t-t_d)} & \text{if } t \geq t_d \end{cases}$$

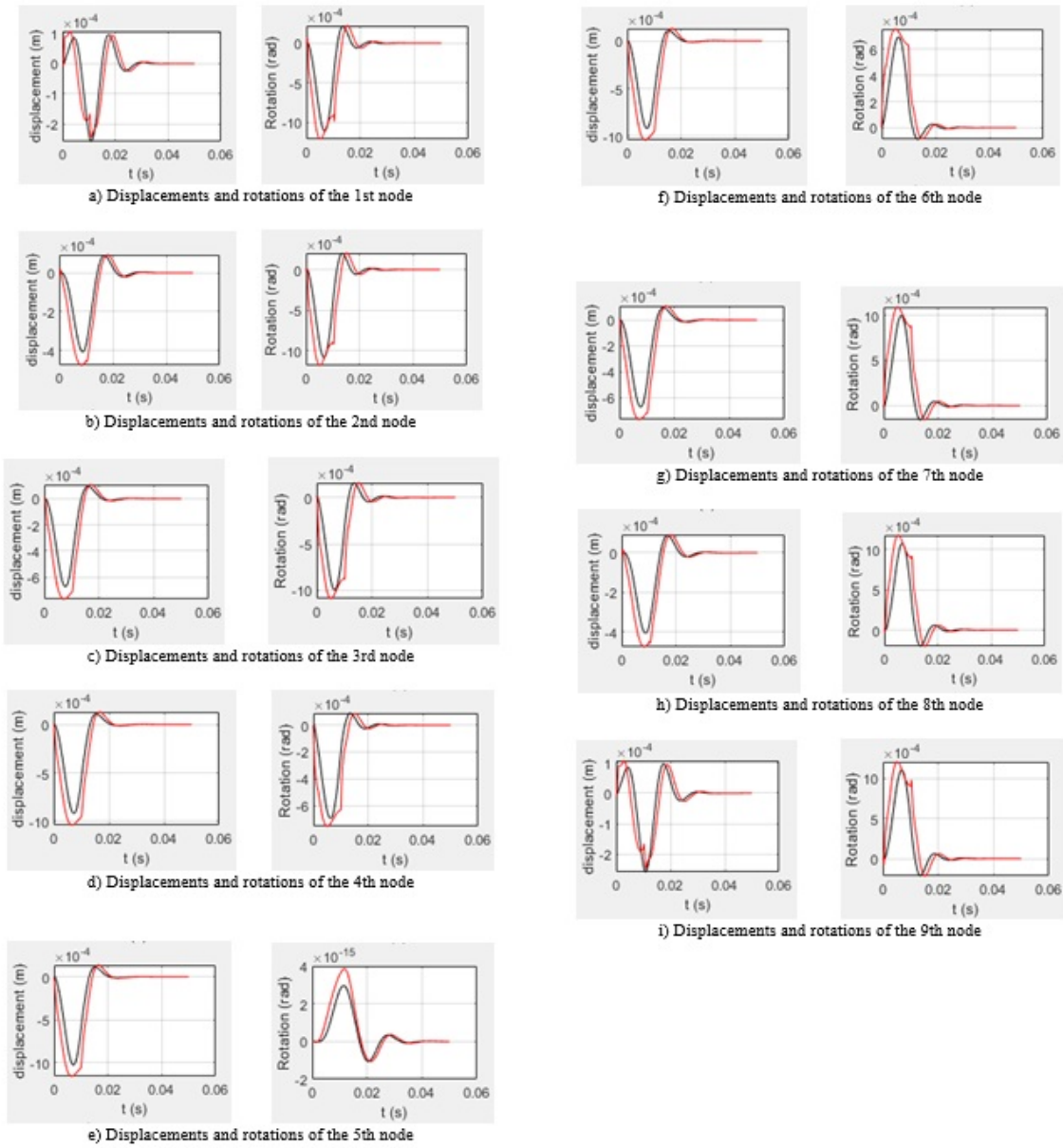


Figure 6: Rail response under sinusoidal, rectangular pulses ($N = 4$, $t_d = 0.01s$, $P = 10T$)

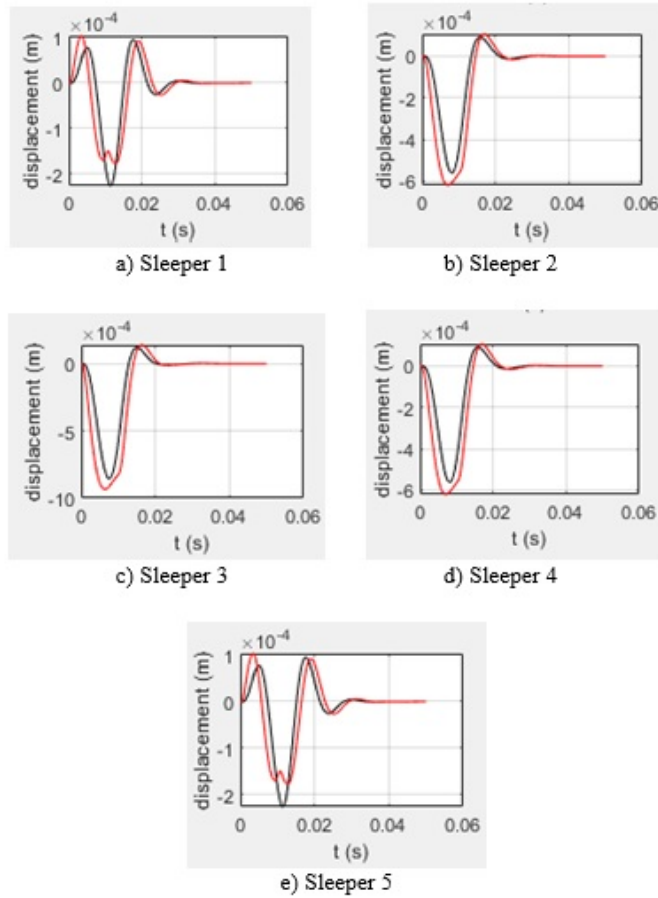


Figure 7: Sleeper response under sinusoidal and rectangular pulses ($N = 4$, $t_d = 0.01s$, $P = 10T$)

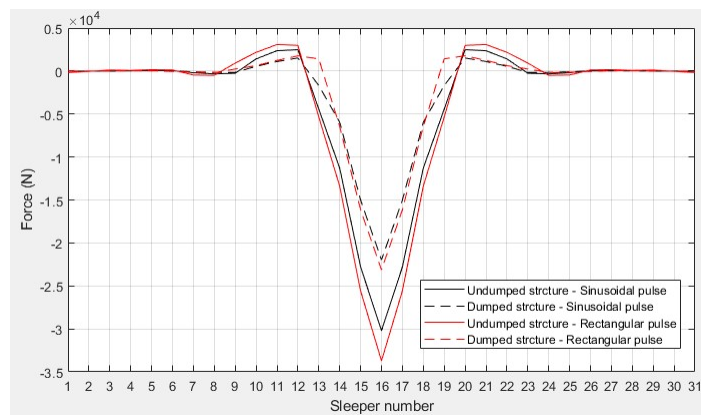


Figure 8: Loads induced in the substructure ($N = 30$, $t_d = 0.01s$, $P = 10T$)

Sleeper number	% of load (undumped - sinusoidal load)	% of load (dumped - sinusoidal load)	% of load (undumped - rectangular load)	% of load (dumped - rectangular load)
13	4.49%	1.73%	5.50%	-
14	11.52%	6.12%	13.66%	6.63%
15	23.24%	15.29%	26.00%	16.41%
16	30.78%	22.43%	34.35%	23.55%
17	23.24%	15.29%	26.00%	16.41%
18	11.52%	6.12%	13.66%	6.63%
19	4.49%	1.73%	5.50%	-

Table 2: Repartition of the loads under the sleepers ($N = 30$, $t_d = 0.01s$, $P = 10T$)

3.3 Results and discussion

The figures presented in this section show the numerical resolution of the system of equations of a dumped track section subjected to a rectangular and sinusoidal loads. The properties of the track are defined in table 1. In figure 6 and figure 7, the sinusoidal pulse is presented in red; however, the rectangular pulse is presented in black.

1. Displacements and rotations of the rail
2. Displacements of the sleepers

It's clear that the maximum values of rail and sleepers movement under rectangular pulse are higher than those reached under a sinusoidal pulse. The figure 8 shows the maximum loads induced in the substructure. The table 2 shows the repartition of the loads under the sleepers.

These results have many consequences in the railway field. Actually, we may optimize railway infrastructure components for example (like ballast height). Moreover, the study is made by considering a static load (10 T). This load is mainly amplified by rail/wheel interaction and train speed [1].

4 Conclusion

Based on the results of the model analysis studied in order to determine the loads induced on the substructure, the following conclusions can be drawn:

- The common modelling of the load applied on the track due to a moving wheel as a rectangular pulse acting in the time sample of a force signal generates a higher rate of movement in the track and over sizes the loads induced in the substructure than a sinusoidal pulse model;

- Dumping matrix has a major influence on reducing the loads induced in the sub-structure. Therefore, it's necessary to preserve the quality of the track components while maintaining it.

As an application, we may evaluate the track behavior according to different characteristics of the track elements that degrade because of maintenance operations. Indeed, the ballast is considered as the most affected element because of operations of damping required for track geometry corrections.

References

- [1] Touati M., Lamdouar N. and Bouyahyaoui A.: Railway vehicle response under random irregularities on a tangent track – nonlinear 3D multi-body modelling. *International Journal of Mechanical Engineering and Technology* 9 (7) (2018) 944–956.
- [2] Xiwen Y., Shaojie G., Shunhua Z., Yao S. and Xiaoyun M.: Vertical Vibration Analysis of Vehicle-Track-Subgrade Coupled System in High Speed Railway with Dynamic Flexibility Method. *Transportation Research Procedia* 25 (2017) 291–300.
- [3] Al Shaer A., Duhamel D., Sab K., Foret G. and Schmitt L.: Experimental settlement and dynamic behavior of a portion of ballasted railway track under high speed trains. *Journal of Sound and Vibration* 316 (1-5) (2008) 211–233.
- [4] M. Kaynia A., Madshus C. and Zackrisson P.: Ground Vibration from High-speed Trains: Prediction and Countermeasure. *Journal of Geotechnical and Geoenvironmental Engineering* 126 (6) (2000) 531–537.
- [5] Takemiya H.: Simulation of Track–ground Vibrations due to High-speed Trains. . Proceedings of the Eighth International Congress on Sound and Vibration. Hong Kong, China (2000) 2875–2882.
- [6] Madshus C. and Kaynia K.: High-speed Railway Lines on Soft Ground: Dynamic Behaviour at Critical Train Speed. *Journal of Sound and Vibration* 231 (3) (2000) 689–701.
- [7] Qian S. and Ying C.: A Spatial Time-Varying Coupling Model for Dynamic Analysis of High Speed Railway Subgrade. *Journal of Southwest Jiaotong University* 14 (5) (2001) 509–513.
- [8] Chebli H., Clouteau D. and Schmitt L.: Dynamic response of high-speed ballasted railway tracks: 3D periodic model and in situ measurements. *Soil Dynamics and Earthquake Engineering* 28 (2) (2008) 118–131.
- [9] Mario P. and William L.: *Structural dynamics: Theory and Computation*. Springer US (2004).
- [10] DIN-EN-13481-1 : Railway applications.Track. Performance requirements for fastening systems Part 1 : Definitions (2012). .
- [11] Kouroussis G., Verlinden O. and Conti C.: Prediction of vibratory nuisances of rail transport vehicles. . 6th National Congress on Theoretical and Applied Mechanics - NCTAM (2003) .
- [12] Zhai W. and Sun X.: A detailed model for investigating vertical interaction between railway vehicle and track. *Vehicle System Dynamics* 23 (Sup1) (1994) 603–615.

Received: February 22, 2021

Accepted for publication: April 10, 2021

Communicated by: Giuseppe Gaeta